JOURNAL

OF THE AMERICAN CHEMICAL SOCIETY

VOLUME 106, NUMBER 12 JUNE 13, 1984

Electronic Structure and Bonding of $Hg(CH_3)_2$, $Hg(CN)_2$, $Hg(CH_3)(CN)$, $Hg(CCCH_3)_2$, and $Au(PMe_3)(CH_3)$

Roger L. DeKock,*[1] Evert Jan Baerends, Paul M. Boerrigter, and Rudy Hengelmolen

Contribution from the Department of Inorganic and Theoretical Chemistry, Free University, De Boelelaan 1083, 1081 HV Amsterdam, The Netherlands. *Received October 24, 1983*

Abstract: In this paper we report the results of our calculations on the title compounds using the LCAO-MO Hartree–Fock–Slater method, including relativistic effects. Excellent agreement is obtained between the computed and experimentally reported ionization potentials for each of the molecules. The results point toward a new assignment of the ultraviolet photoelectron spectra in the region of the d^{10} ionization bands. In particular, an ionization event from an orbital that contains a large component of d_σ is stabilized in all of the compounds except $Hg(CH_3)_2$, relative to the spin–orbit components composed mainly of the d_π and d_δ orbitals. The net contribution of the metal d electrons to the overall bonding is only about 10% for the Hg compounds but approaches 40% for the Au–PH_3 bond of the model compound $Au(PH_3)(CH_3)$. Calculations also have been carried out without the use of 6p orbitals to show that these orbitals contribute only slightly to the bond strength. The picture that emerges is that at least 80% of the bonding for the Hg compounds is due to the 6s orbital on the Hg atom, and hence the bonding is best described in terms of a three-center two-electron bond. This description is shown to be in agreement with the known relative bond strengths of group 2 metal halides MX_2, wherein removal of the first X atom to form MX requires much more energy than the removal of the second X atom.

The electronic structure and bonding of $Hg(CH_3)_2$ and of the mercury halides HgX_2 have been studied extensively. For example, the ultraviolet photoelectron (UP) spectra of these compounds have been reported by several research groups,[2] and theoretical molecular orbital studies also have been completed.[3] Nevertheless, due to the complications of relativistic effects it is difficult to assign the experimental UP spectra and to determine their bearing on bonding issues, so it cannot be said that the overall bonding is well understood for Hg(II) compounds.

It is the purpose of this work to examine thoroughly the nature of the bonding for the title compounds using the Hartree–Fock–Slater (HFS) method[4] including relativistic effects in our study.[5] This method has been shown in a number of studies to give reliable computed ionization potentials, for systems involving light[6] and heavy atoms.[7] As such the method can serve as a useful tool for the assignment of UP spectra, particularly where substituent and relative intensity effects do not make the assignment obvious from an experimental viewpoint. In addition to comparing computed ionization energies with those that have been experimentally reported, we intend to study the importance of relativistic effects. In the second part of the paper we examine the bonding in the title compounds, in particular the relative importance of the various valence orbitals on the metal toward the bonding with the ligands.

The basic picture of the σ bonding is presented in Figure 1, at both the nonrelativistic and the relativistic level. In all of our discussion, we choose the z axis to be the axis of highest fold symmetry, and we use the terminology of $D_{\infty h}$ symmetry whenever it is convenient (σ,π,δ). Let us first consider the nonrelativistic interaction diagram. Bonding interactions with the metal atom can take place via the 6s, $6p_\sigma$, and $5d_\sigma$ orbitals. Since the 6p orbital lies some 5 eV above the 6s orbital for atomic Hg,[8] its involvement in the overall bonding is problematic. Although the 6p orbital often is invoked in terms of an sp hybrid bonding model,[9] an analysis of the results of an HFS calculation on HgI_2 (3a) seemed

(1) Current address: Department of Chemistry, Calvin College, Grand Rapids, MI 49506.

(2) (a) Eland, J. H. D. *Int. J. Mass Spectrom. Ion Phys.* **1970**, *4*, 37. (b) Boggess, G. W.; Allen, J. D., Jr.; Schweitzer, G. K. *J. Electron Spectrosc. Relat. Phenom.* **1973**, *2*, 467. (c) Fehlner, T. P.; Ulman, J.; Nugent, W. A.; Kochi, J. K. *Inorg. Chem.* **1976**, *15*, 2544. (d) Coatsworth, L. L.; Bancroft, G. M.; Creber, D. K.; Lazier, R. J. D.; Jacobs, P. W. M. *J. Electron Spectrosc. Relat. Phenom.* **1978**, *13*, 395. (e) Bancroft, G. M.; Creber, D. K.; Basch, H. *J. Chem. Phys.* **1977**, *67*, 4891. (f) Creber, D. K.; Bancroft, G. M. *Inorg. Chem.* **1980**, *19*, 643.

(3) (a) Snijders, J. G.; Baerends, E. J.; Ros, P. *Mol. Phys.* **1979**, *38*, 1909. (b) Tse, J. S.; Bancroft, G. M.; Creber, D. K. *J. Chem. Phys.* **1981**, *74*, 2097.

(4) Baerends, E. J.; Ros, P. *Int. J. Quantum Chem., Quantum Chem. Symp.* **1978**, *No. 12*, 169. Heijser, W.; Baerends, E. J.; Ros, P. *Faraday Discuss. Chem. Soc.* **1980**, *No. 14*, 211. Famiglietti, C.; Baerends, E. J. *Chem. Phys.* **1981**, *62*, 407.

(5) (a) Snijders, J. G.; Baerends, E. J.; Ros, P. *Mol. Phys.* **1979**, *38*, 1909. (b) Ziegler, T.; Snijders, J. G.; Baerends, E. J. *J. Chem. Phys.* **1981**, *74*, 1271.

(6) Baerends, E. J.; Ros, P. *Chem. Phys.* **1973**, *2*, 52.

(7) Jonkers, G.; Van der Kerk, S. M.; Mooyman, R.; De Lange, C. A.; Snijders, J. G. *Chem. Phys. Lett.* **1983**, *94*, 585. Hitchcock, A. P.; Hao, N.; Werstiuk, N. H.; McGlinchey, M. J.; Ziegler, T. *Inorg. Chem.* **1982**, *21*, 793.

(8) (a) Cotton, F. A.; Wilkinson, G. "Advanced Inorganic Chemistry", 4th ed.; New York: Wiley, 1980; p 590. (b) Moore, C. E. "Atomic Energy Levels", National Bureau of Standards, Circular 467, 1949, Vol. I, 1952, Vol. II, 1958, Vol. III.

(9) Purcell, K. F.; Kotz, J. C. "Inorganic Chemistry"; Saunders Publishing Co.: Philadelphia, 1977; p 120.

0002-7863/84/1506-3387$01.50/0

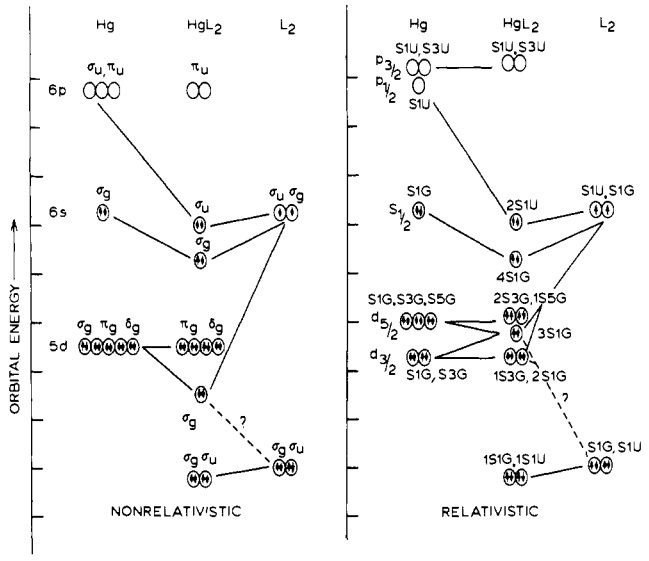

Figure 1. Schematic energy level diagrams for linear HgL_2 where L is a ligand that has three σ electrons. Depending upon the ligand, the low-lying σ orbital might interact strongly or weakly with the Hg $5d_\sigma$ orbital and hence this interaction is indicated with a question mark.

to indicate that there was little participation by the 6p orbitals in the bonding.

The extent of 5d orbital bonding also is rather unknown. The ionization pattern of the Hg "$5d^{10}$" electrons in the region of 15–17 eV at first glance appears to be very atomic-like, exhibiting a spin–orbit splitting between $5d_{5/2}$ and $5d_{3/2}$ bands, at least for HgX_2 and $Hg(CH_3)_2$. In order to understand the ionization pattern in the d region, we turn to the right side of Figure 1, which presents the interaction diagram at the relativistic level. The notation that we employ for $D_{\infty h}$ molecules is S1G, S1U, S3G, S3U, ..., where the letter following S is twice the $|m_j|$ value of the state. The letters G or U show the effect of the inversion operation. We do not draw all possible correlations in the diagram. Suffice it to say that the situation is more complicated than that presented at the nonrelativistic level. In principal, we can have five different ionization events for the d electrons: S1G, S1G, S3G, S3G, and S5G. For $Hg(CH_3)_2$, the latest interpretation of the experimental results[2d] assigns a band at 15.0 eV to S3G and S5G, a weaker band at 15.4 eV to S1G, and the third band at 16.9 eV to S1G and S3G. Such an assignment is understandable on the basis of the interaction diagram presented in Figure 1, where a high-lying ligand orbital of S1G symmetry interacts more strongly with the metal d orbitals than does the low-lying S1G orbital. The position of the 3S1G peak (often denoted $^2\Sigma_{1/2}$) has been used to monitor the d_σ involvement in bonding: simple crystal-field considerations put d_σ above d_π, d_δ, so the reverse ordering indicates stabilization of d_σ by covalent bonding effects.[2,10,11] However, the relative position of the 3S1G ionization event by itself does not provide much insight into the amount of d_σ involvement in the bonding. This is due to the presence of relativistic effects and the possible involvement of low-lying ligand σ orbitals on the bonding (indicated by a ? in Figure 1). What is meant by relativistic effects is primarily the *mixing* of the different d orbitals by the spin–orbit effect. Due to spin–orbit coupling the S1 representation contains both d_σ and d_π components. Relativistic effects also include the *shifting* of the levels brought about by various terms (mass velocity, Darwin, etc.) that will be discussed later.

We recently have become interested in the electronic structure and bonding of $Hg(CN)_2$ and $Hg(CCCH_3)_2$ as a result of our work on the related $M(PR_3)_2(CN)_2$ and $M(PR_3)_2(CCCH_3)_2$ compounds where M = Pd and Pt.[12] Comparatively less experimental and theoretical work has been done on these mercury compounds than on $Hg(CH_3)_2$ and HgX_2. The UP spectra of both compounds and of $Hg(CH_3)(CN)$ have been reported.[10] For $Hg(CN)_2$ and $Hg(CH_3)(CN)$ only the $5d^{10}$ ionization events in the region around 16–20 eV have been published. On the theoretical side a discrete-variational-Xα calculation on $Hg(CN)_2$ has been carried out by Sano et al.,[13] but this calculation did not make reference to the UP work nor were relativistic corrections considered. In view of the relatively complicated ionization pattern in the $5d^{10}$ region, we considered it worthwhile to examine the bonding in $Hg(CN)_2$, $Hg(CH_3)(CN)$, and $Hg(CCCH_3)_2$. It should be remarked that the ligand systems $CCCH_3$ and CN are very similar since CCH is isoelectronic with CN. Therefore, any unusual features in the bonding of one of these Hg compounds also should be exhibited in the other.

Recently the He(I) and He(II) UP spectra of $Au(PMe_3)(CH_3)$ have been reported and Xα-SW calculations on the model compound $Au(PH_3)(CH_3)$ have been completed.[11] Since the latter molecule has the same number of valence electrons as $Hg(CH_3)_2$, it should provide insight into the overall bonding picture for the mercury compounds. For this and the other molecules the assigned spectrum of $Hg(CH_3)_2$ has served as a model in making the empirical assignment of the spectra. One objective of our work was to determine from the calculations if $Hg(CH_3)_2$ does serve as a respectable model for the other molecules. In principal, d orbital involvement should be more important for Au compounds than for Hg compounds because the Au 5d orbitals are destabilized about 4 eV compared to Hg.[8] Hence the Au 5d orbitals are much more "valence-like" than the more "core-like" Hg 5d orbitals. The actual extent of 5d orbital involvement in Au vs. Hg compounds is not known. Bancroft et al.[11] have interpreted the UP spectrum of $Au(PMe_3)(CH_3)$ to indicate that Au 5d orbitals are involved in bonding only slightly more than Hg 5d orbitals, and Mason[14] has concluded from studies on the optical spectrum of $Au(CN)_2^-$ that Au 5d orbitals are not strongly involved in bonding to the CN ligand. Because of our interest in comparative 5d orbital involvement for Hg and Au, we decided to include $Au(PMe_3)(CH_3)$ in our study.

Calculations

We have carried out calculations on $Hg(CH_3)_2$, $Hg(CN)_2$, $Hg(CH_3)(CN)$, $Hg(CCCH_3)_2$, and $Au(PH_3)(CH_3)$. In each case a linear framework of the non-hydrogen atoms was assumed in either $D_{\infty h}$, C_{3v}, or D_{3h} symmetry. We also have carried out a calculation on $Au(PMe_3)(CH_3)$ in order to determine the effects of PMe_3 compared to PH_3 on the computed ionization potentials and on the overall conclusions about the bonding. For all the calculations the bond angles within the methyl group were taken to be tetrahedral, and the C–H bond length was fixed at 1.09 Å. Our chosen Hg–CH_3 bond length is the same as that taken by Tse et al.[3b] in their study of $Hg(CH_3)_2$. For $Hg(CN)_2$ we employed an Hg–CN bond length of 2.0 Å and a CN bond length of 1.16 Å, close to those used by Sano et al.[13] in their study of $Hg(CN)_2$. The bond lengths chosen within the propynyl ligand are in accord with known crystallographic X-ray results for this and related ligands:[15,16] C–C of 1.20 Å and C–CH_3 of 1.46 Å. The P–C–P bond angles were chosen to be 105° and a P–C bond length of 1.82 Å was used, in agreement with the structure of this ligand system when coordinated to an oxygen atom.[17] The same bond angle was chosen for the H–P–H bond in the PH_3 model

(10) (a) Burroughs, P.; Evans, S.; Hamnett, A.; Orchard, A. F.; Richardson, N. V. *J. Chem. Soc., Chem. Commun.* **1974**, 921. (b) Furlani, C.; Piancastelli, M. N.; Cauletti, C.; Faticanti, F.; Ortaggi, G. *J. Electron Spectrosc. Relat. Phenom.* **1981**, *22*, 309.

(11) Bancroft, G. M.; Chan, T.; Puddephatt, R. J.; Tse, J. S. *Inorg. Chem.* **1982**, *21*, 2946.

(12) Louwen, J. N.; Hengelmolen, R.; Grove, D. M.; Oskam, A.; DeKock, R. L. *Organometallics*, in press.

(13) Sano, M.; Adachi, H.; Yamatera, H. *Bull. Chem. Soc. Jpn.* **1982**, *55*, 1022.

(14) Mason, W. R. *J. Am. Chem. Soc.* **1976**, *98*, 5182.

(15) (a) "Handbook of Chemistry and Physics", 58th ed.; CRC Press: Cleveland, 1977. (b) Pedley, J. B.; Rylance, J. "Computer Analysed Thermochemical Data of Organic and Organometallic Compounds"; University of Sussex: Sussex, England, 1977.

(16) Nast, R. *Coord. Chem. Rev.* **1982**, *47*, 89.

(17) Wilkins, C. J.; Hagen, K.; Hedberg, L.; Shen, Q.; Hedberg, K. *J. Am. Chem. Soc.* **1975**, *97*, 6352.

Table I. Symmetry Relations between Central Atom Basis Orbitals in the Various Groups and Double Groups

R_3	R_3*	$D_{\infty h}$	$D_{\infty h}$*	D_{3h}	D_{3h}*	C_{3v}	C_{3v}*
s	$s_{1/2}$	σ_g	S1G	a_1'	S1	a_1	S1
p	$p_{1/2}$, $p_{3/2}$	σ_u	S1U	a_2''	S5	a_1	S1
		π_u	S1U, S3U	e'	S3, S5	e	S1, S3
d	$d_{3/2}$, $d_{5/2}$	σ_g	S1G	a_1'	S1	a_1	S1
		π_g	S1G, S3G	e''	S1, S3	e	S1, S3
		δ_g	S3G, S5G	e'	S3, S5	e	S1, S3

Table II. Mulliken Population Analysis for the Occupied Orbitals of $Hg(CH_3)_2$[a]

orbital	ionization energy	percent character[b] Hg	CH_3
$1a_1'$	19.30	5.3 6s	78.2 $1a_1$
		14.7 5d	
$2a_1'$	16.15	75.3 5d	16.9 $1a_1$
			7.0 $2a_1$
$3a_1'$	9.22	56.9 6s	38.0 $2a_1$
		5.3 5d	
$1a_2''$	18.72		99.3 $1a_1$
$2a_2''$	8.09	7.3 6p	88.7 $2a_1$
1e'	17.15	99.9 5d	
2e'	11.85		99.5 1e
1e''	17.39	93.3 5d	6.6 1e
2e''	11.40	6.6 5d	93.0 1e

[a] Transition-state ionization energies (eV) are without relativistic corrections. [b] Occupations: Hg, $(5d_\delta)^{2.00}(5d_\pi)^{2.00}(5d_\sigma)^{1.91}(6s)^{1.24}(6p_\pi)^{0.01}(6p_\sigma)^{0.08}$; CH_3, $(1a_1)^{1.97}(2a_1)^{1.35}(1e)^{2.00}$. Fragment charges: Hg, +0.55; CH_3, −0.27.

ligand. The P–H bond length was taken to be the same as in free PH_3.[15] The Au–P and Au–C bond lengths were the same as those chosen by Bancroft et al.[11]

The calculations reported in this work were carried out utilizing the HFS method developed in these laboratories.[4-7] The basis set was double ζ including double ζ 6p polarization functions on the Hg atom, single ζ 2p orbitals on the H atoms (ζ = 1.0), and single ζ 3d on the P atom (ζ = 1.3). The cores Au(1s–5p), Hg(1s–5p), C(1s), N(1s), and P(1s–2p) have been kept frozen. In the calculation of ionization energies, we have employed either the Slater transition-state method or the ΔSCF method using the Ziegler transition-state energy.[18] Either method gives identical results to within a few hundredths of an electron volt. The latter energy analysis also allows us to compute binding energies between fragments in terms of a steric interaction term and an electronic interaction term.

We also have carried out calculations with 5d orbitals in the core to examine the effect of the 5d orbitals on the binding energy. The effect of the 6p orbitals on the binding was determined both by their contribution to the bond energy and by removing 6p orbitals from the basis set.

In order to simplify the subsequent discussion, we present in Table I a correlation diagram for the metal atom orbitals in the various point groups that we employ, both single groups and double groups.

Results and Discussion

(A) Comparison with the Photoelectron Spectra and Discussion of the Importance of Relativistic Effects. (1) $Hg(CH_3)_2$. We begin our discussion with $Hg(CH_3)_2$, the most well-understood molecule of the series. A ground-state energy level diagram is presented in Figure 2, calculated at the nonrelativistic level. Also presented in Figure 2 are the calculated transition-state ionization energies and the shifts in these values brought about by relativistic effects.

(18) Ziegler, T.; Rauk, A. *Theor. Chim. Acta* **1977**, *46*, 1. Ziegler, T.; Rauk, A. *Inorg. Chem.* **1979**, *18*, 1558, 1755. Baerends, E. J.; Post, D. In "Quantum Theory of Chemical Reactions"; Daudel, R., Pullman, A., Salem, L., Veillard, A., Eds.; Reidel: Dordrecht, The Netherlands, 1982; Vol. III, p 15.

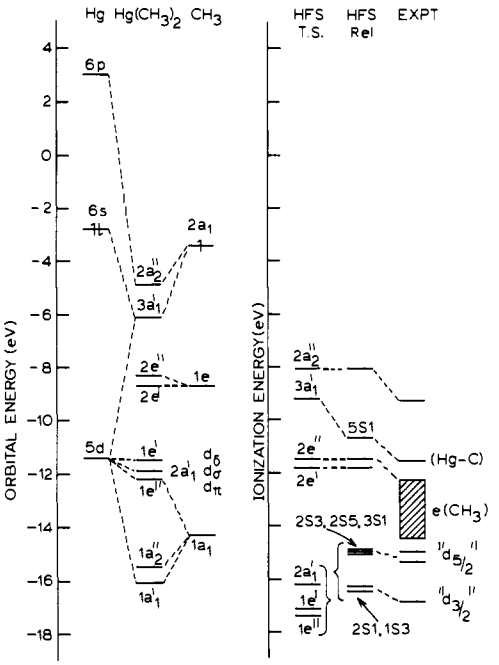

Figure 2. Orbital energy level diagram for $Hg(CH_3)_2$ obtained from the HFS calculations. On the right we present the calculated ionization energies obtained by using the transition-state method (HFS-TS) and with the relativistic corrections (HFS-rel). These results are then further compared with experiment. The ionization energy scale is the same as the orbital energy scale except for a change in sign. The energy levels presented for Hg and CH_3 are those calculated for these starting levels in the molecular field.

Table III. Summary of Nonrelativistic and Relativistic HFS Calculations for Five Orbitals of $Hg(CH_3)_2$ that Undergo Significant Relativistic Shifts[a]

	nrel	Δ_{MV}	Δ_{DAR}	Δ_{SO}	Δ_{SO}^{ind}	Δ_{POT}	rel	rel state
				$Hg(CH_3)_2$				
$3a_1'$	−9.22	−4.80	2.58	0.00	−0.12	0.87	−10.69	5S1
$2a_1'$	−16.15	−1.22	−0.10	0.00	+0.47	2.11	−14.89	3S1
1e'	−17.15	−1.93	−0.02	0.66	−0.08	3.54	−14.98	2S5
		−1.93	−0.02	−0.66	−0.37	3.61	−16.52	1S3
1e''	−17.39	−2.01	0.18	0.28	0.33	3.52	−15.09	2S3
		−2.01	0.18	−0.28	−0.51	3.68	−16.32	2S1
				Hg Atom				
s	−7.70	−4.76	2.65	0.0		0.70	−9.11	$S_{1/2}$
d	−16.90	−1.98	0.01	−1.02		3.52	−16.37	$D_{3/2}$
		−1.98	0.01	0.67		3.60	−14.60	$D_{5/2}$

[a] Given are nonrelativistic transition-state energies (nrel) and corrections due to the relativistic increase of mass with velocity (Δ_{MV}), Darwin correction (Δ_{DAR}), direct (diagonal) spin–orbit interaction (Δ_{SO}), indirect (off-diagonal) spin–orbit interaction (Δ_{SO}^{ind}), and relativistic change in the electronic potential (Δ_{POT}). In the final columns the total relativistic energies are given and assigned.

Upon introduction of the relativistic shifts the overall agreement between experiment and theory is excellent.

In Table II we present a Mulliken population analysis of the nonrelativistic orbitals. We note that there is little mixing between Hg AOs and CH_3 orbitals in any of the MOs except $3a_1'$. This penultimate MO consists mainly of Hg 6s and the frontier hybrid orbital of CH_3 ($2a_1$). There is only small occupation of the 6p orbitals; the 5d orbitals are nearly completely occupied. Only d_σ is significantly less than 2.0, and it has an occupation of 1.9 electrons. The overall picture that emerges is that the bonding is mainly brought about by the Hg 6s–CH_3 $2a_1$ interaction in the $3a_1$ orbital, but this effect will be examined more thoroughly in the section on bonding contributions (section B).

We examine the relativistic effects more closely in Table III, where we present a breakdown of the relativistic terms for the

Table IV. Percent Analysis of the Relativistic Spinors for the Ground-State Calculation on $Hg(CH_3)_2$ and Hg Atom[a]

Hg atom spinor	$\|m_j\|$	contributions in percent				
		d_σ	d_{π_1}	d_{π_2}	d_{δ_1}	d_{δ_2}
$D_{5/2}$	$^5/_2$				50	50
	$^3/_2$		40	40	10	10
	$^1/_2$	60	20	20		
$D_{3/2}$	$^3/_2$		10	10	40	40
	$^1/_2$	40	30	30		

$Hg(CH_3)_2$ spinor	contributions in percent					
	$2a_1'$	$3a_1'$	$1e_1''$	$1e_2''$	$1e_1'$	$1e_2'$
2S1	39.6	0.9	29.1	29.1		
3S1	55.2	2.3	20.8	20.8		
5S1	2.3	90.5			0.1	0.1
1S3			25.7	25.7	23.7	23.7
2S3			21.8	21.8	26.0	26.0
2S5					49.6	49.6

[a] Each column contains the sum of α and β spin–orbital contributions.

four orbitals that exhibit the largest effects due to relativity. Also presented in Table III are the relativistic corrections for the Hg atom. The composition of the MOs is reflected in the relativistic corrections. For example, the 1e′ and 1e″ MOs, being almost pure 5d (Table II), have mass–velocity corrections close to the atomic one; the $2a_1'$ (d_σ) has smaller corrections due to its stronger mixing with the ligand orbitals. Notice from Figure 2 and Table III that the relativistic shift in the $3a_1'$ orbital is necessary to reproduce the experimental splitting between the two Hg–C ionization events ($3a_1'$ and $2a_2''$). The relativistic stabilization of $3a_1'$ is brought about by the mass–velocity correction and is due to the 57% 6s character in this orbital.

We next turn our attention to the $2a_1'$ orbital, which is mainly Hg 5d. Of all the mainly 5d MOs, it is this orbital that has most captured the imagination of chemists because it exhibits the largest effects due to bonding with ligand orbitals. Notice from Table II that $2a_1'$ contains not only bonding components with CH_3 $2a_1$ but also antibonding components with the $1a_1$ orbital of CH_3. The net result is that $2a_1'$ is both "pushed from above" and "pushed from below" so that at the nonrelativistic level it lies close to the other mainly 5d MOs (1e′ and 1e″), as seen in Figure 2. If we have, as in this case, levels of the same double group symmetry lying close to each other, the spin–orbit (SO) operator will couple these. If the d_σ, d_π, and d_δ levels were purely atomic and strictly degenerate this coupling would of course restore the $d_{5/2}$ and $d_{3/2}$ atomic spinors. In Table III we distinguish between the first-order SO shift in the nonrelativistic levels (the diagonal elements of the SO operator) and the additional shift due to the coupling (the off-diagonal or indirect Δ_{SO}^{ind}). Only if the ligand field splitting of the nonrelativistic levels is large compared to the off-diagonal elements (which are of the same order as the atomic SO splitting) may we ignore the molecular SO coupling (see ref 3a for an extensive discussion of the analogous HgI_2 case). This point will be a recurrent theme in our discussion of the 5d region of the title compounds.

For $Hg(CH_3)_2$ we examine more carefully the nature of the relativistic orbitals by a percent analysis in Table IV of the ground-state spinors that were given in Table III. Notice that spinor 3S1 contains 55% $2a_1'$, 21% $1e_1''$, and 21% $1e_2''$. (The subscripts 1 and 2 refer to the degenerate components of the nonrelativistic orbitals of e″.) Since $2a_1'$ is 75% d_σ (Table II), and the 1e″ orbitals are nearly pure d_{xz} and d_{yz}, spinor 3S1 corresponds to about 40% d_σ, 20% d_{xz}, and 20% d_{yz}. Except for the "dilution" of the d_σ orbitals in the $2a_1'$ MO (75%), this spinor is close in character to the $|m_j| = {}^1/_2$ component of $d_{5/2}$ of atomic Hg. Likewise, 2S1 corresponds to the $|m_j| = {}^1/_2$ component of the $d_{3/2}$ spinor of atomic Hg.

The 2S5 spinor corresponds directly to the $|m_j| = {}^5/_2$ component of the $d_{5/2}$ state of atomic Hg. However, analysis of spinors 1S3 and 2S3 shows that they have a different distribution of d character than do the corresponding $d_{5/2}$ and $d_{3/2}$ ($|m_j| = {}^3/_2$) states of atomic Hg. The reason that the S1 spinors correlate strongly with the corresponding atomic state whereas the S3 spinors do not is readily apparent from the ground-state energy level diagram presented in Figure 2. Notice that the 1e″ and $2a_1'$ orbitals are nearly degenerate as they were (exactly) in the free atom. Hence, these states will couple through the SO operator as though they were atomic in character. However, the 1e′ and 1e″ orbitals are split by 0.6 eV and therefore exhibit much more divergence from the atomic distribution of d character for the S3 states.[19] In summary, the $5d^{10}$ region of the photoelectron spectrum of $Hg(CH_3)_2$ *appears* to be atomic-like, but we find that the situation is somewhat more complicated.

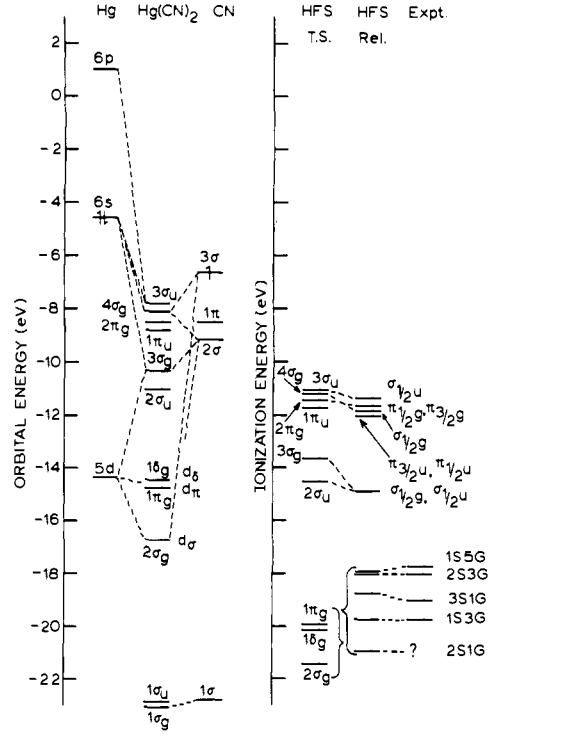

Figure 3. Orbital energy level diagram and calculated ionization energies for $Hg(CN)_2$. The unobserved ionization events in starting levels in the valence region are labeled in the traditional way since they involve less relativistic mixing.

The calculation places the lower d-type (3S1) ionization event at 14.9 eV, slightly lower than the experimentally assigned position at about 15.4 eV.[2d] However, there is no a priori reason to choose one assignment over another among these three closely spaced ionization events (3S1, 2S3, and 2S5). In any case, due to spin–orbit mixing of the 5d orbitals it is not possible to refer to any single one of the 5d ionization events as being due to $5d_\sigma$ as is often done.[2,10,11]

(2) $Hg(CN)_2$. We turn next to the energy level diagram and computed ionization energies for $Hg(CN)_2$ (Figure 3). The reported He(I) UP spectrum[10a] is very rich in the $5d^{10}$ region (17–20 eV), exhibiting four of the five bands that might be expected in the presence of the linear framework and the relativistic effects. Our assignment is quite different in the d-band region than that arrived at by reference to $Hg(CH_3)_2$.[10a] The major change in the assignment is that we now place the 2S1G ionization event (containing a large component of d_σ), at 20.9 eV, rather than at ~18 eV—a shift of almost 3 eV!

The reasons for this differential shift of the $5d_\sigma$ orbital are readily apparent by comparing Figures 2 and 3. The CN ligand presents three σ orbitals rather than the two orbitals ($1a_1$ and $2a_1$)

(19) This argument uses the ground-state 1-electron energies as depicted in Figure 2, which exhibit a different ordering and spacing than the IE's (equal to transition-state 1-electron energies) in Table III. Any *given* transition-state calculation, however, has a level spacing similar to that given by the ground state, indicating the ground-state analysis to be adequate. Spinor analyses we have carried out on selected transition states confirmed this.

Table V. Mulliken Population Analysis for the Occupied Orbitals of $Hg(CN)_2$[a]

orbital	ionization energy	percent character[b] Hg	CN
$1\sigma_g$	25.61		99.9 1σ
$2\sigma_g$	21.38	75.4 d	8.1 2σ
			9.6 3σ
$3\sigma_g$	13.60	33.6 6s	39.6 2σ
		19.6 5d	5.8 3σ
$4\sigma_g$	11.17	13.7 6s	43.4 2σ
			43.0 3σ
$1\sigma_u$	25.89		102 1σ
$2\sigma_u$	14.45	3.7 6p	68.1 2σ
			23.7 3σ
$3\sigma_u$	11.06	5.6 6p	31.8 2σ
			61.9 3σ
$1\pi_g$	19.95	97.3 5d	
$2\pi_g$	11.40		97.8 1π
$1\pi_u$	11.70		99.3 1π
$1\delta_g$	20.08	100 5d	

[a] Same as footnote *a* in Table II. [b] Occupations: Hg, $(5d_\delta)^{2.00}(5d_\pi)^{1.99}(5d_\sigma)^{1.93}(6s)^{1.03}(6p_\pi)^{0.00}(6p_\sigma)^{0.14}$; CN, $(1\sigma)^{1.99}(2\sigma)^{1.91}(3\sigma)^{1.44}(1\pi)^{1.99}(2\pi)^{0.01}$. Fragment charges: Hg, +0.75; CN, −0.38.

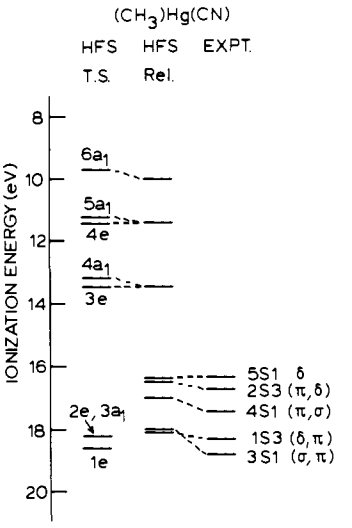

Figure 4. Correlation between theory and experiment for $(CH_3)HgCN$. In the assignment of the 5d derived bands, the predominant character is that indicated first.

of CH_3. However, the 1σ level of CN is so low in energy as to alleviate any "pushing-from-below" effect as observed for $Hg(CH_3)_2$. Also the d_σ level interacts strongly with both 2σ and 3σ; both of these ligand orbitals have a strong overlap with the Hg 5d orbital. (See ref 13 for contour diagrams of the CN fragment orbitals). Furthermore, the 5d level is closer to 2σ of CN than to $2a_1$ of CH_3 so the "pushing-from-above" effect is larger for $Hg(CN)_2$ than for $Hg(CH_3)_2$. Finally, the 3S1 ("$5d_\sigma$") level of $Hg(CH_3)_2$ was shifted relativistically by about 1 eV to lower ionization energy whereas 2S1G of $Hg(CN)_2$ is shifted by only about 0.5 eV (vide infra). According to our prediction then, the 2S1G ($5d_\sigma$) ionization event of $Hg(CN)_2$ has not been observed yet, and He(II) photoelectron spectra will be required for its detection.

The Mulliken population analysis (Table V) bears out the qualitative analysis obtained from Figure 3. In addition, we see that there is very little π^* back-bonding to the CN ligand. The CN ligand gains more charge in its upper σ level than does CH_3, and this had tended to shift the whole $5d^{10}$ pattern to higher ionization energy by 2–3 eV, as observed experimentally.

In Table VI we present a breakdown of the orbitals that exhibit important relativistic effects for $Hg(CN)_2$, and in Table VII is given the corresponding percent analysis of the spinors. The values show that the 2S1G orbital correlates almost purely with the $2\sigma_g$ nonrelativistic orbital. The reason for lack of spin–orbit coupling with the $1\pi_g$ orbital is that the CN ligands have induced such a strong bonding interaction with the $2\sigma_g$ orbital as to drive it 2 eV below the $1\pi_g$ orbital at the nonrelativistic level (Figure 3). The picture is now quite different than that for $Hg(CH_3)_2$. The 2S1G and 3S1G do not at all correspond to the $|m_j| = {}^1/_2$ components of $d_{3/2}$ and $d_{5/2}$ as they did for $Hg(CH_3)_2$. It appears as if the ligand field effect of the CN ligands has been sufficient to "turn-off" the spin–orbit coupling of the d_σ and d_π states.

On the other hand, the S3 d-type states are *more* atomic-like for $Hg(CN)_2$ than they were for $Hg(CH_3)_2$. This feature could be expected from Figure 3, since the $1\pi_g$ and $1\delta_g$ orbitals are nearly degenerate, and hence they will couple strongly via the spin–orbit effect. Finally, the S5G d-type state is nearly pure atomic-like, as expected. As seen in Figure 3, the lowest of the d-type IEs is assigned to this 1S5G state. This also happens to be the sharpest band in the UP spectrum. Thus the calculation agrees with the experimentally favored assignment for this band.[10a]

The perturbation terms presented in Table VI show why the orbital that contains the major component of d_σ (2S1G) for $Hg(CN)_2$ undergoes a lesser relativistic destabilization than the corresponding orbital (3S1) of $Hg(CH_3)_2$. The major difference between the two lies in the "indirect" spin–orbit effect, which is negative for 2S1G of $Hg(CN)_2$ but positive for 3S1 of $Hg(CH_3)_2$. This change in sign of the indirect spin–orbit effect is a direct consequence of the different bonding characteristics of the CN and CH_3 ligands. Since $2a_1$ lies *above* 1e″ for $Hg(CH_3)_2$, the indirect spin–orbit effect for the upper S1 component will of necessity be positive. For $Hg(CN)_2$ the reverse is true since the $2\sigma_g$ level lies *below* the $1\pi_g$ orbital. Since the indirect spin-orbit effect results from diagonalization of the spin-orbit matrix, this change in sign can readily be understood in terms of second-order perturbation language (e.g., pushing from above vs. pushing from below).

The reported UP spectrum doe not present the low ionization region. Our results for this region also are included in Figure 3 and Table VI. Briefly, we predict the lowest ionization event to be of nitrogen lone pair character but with CN π ionization events lying nearby in energy. We also have carried out broken symmetry ($C_{\infty v}$) calculations on these valence ionization energies. Although the computed ionization energies shift to higher energy by about 1 eV, there is no "crossing over" of calculated ionization events as found for $Se(CN)_2$.[20]

Table VI. Summary of Nonrelativistic and Relativistic HFS Calculations for Orbitals of $Hg(CN)_2$[a]

	nrel	Δ_{MV}	Δ_{DAR}	Δ_{SO}	Δ_{SO}^{ind}	Δ_{POT}	rel	rel state
$3\sigma_g$	−13.60	−3.63	1.55	0.00	−0.11	0.95	−14.84	6S1G
$2\sigma_g$	−21.38	−1.66	0.09	0.00	−0.41	2.42	−20.94	2S1G
$1\pi_g$	−19.95	−1.91	0.02	0.25	+0.41	3.25	−17.93	2S3G
		−1.91	0.02	−0.25	+0.06	3.27	−18.76	3S1G
$1\delta_g$	−20.08	−2.09	0.04	0.72	−0.06	3.51	−17.96	1S5G
		−2.09	0.04	−0.72	−0.40	3.56	−19.69	1S3G

[a] Footnotes as in Table III.

Table VII. Percent Analysis of the Relativistic Spinors for the Ground-State Calculation on $Hg(CN)_2$

	contributions in percent						
spinor	$2\sigma_g$	$3\sigma_g$	$4\sigma_g$	$1\pi_{g1}$	$1\pi_{g2}$	$1\delta_{g1}$	$1\delta_{g2}$
2S1G	92.7	4.9		1.1	1.1		
3S1G	3.4	2.3	0.0	47.0	47.0		
6S1G	0.3	2.2	96.8	0.1	0.1		
1S3G				16.9	16.9	33.0	33.0
2S3G				32.7	32.7	17.0	17.0
1S5G						49.9	49.9

(3) $Hg(CH_3)(CN)$. The UP spectrum of $Hg(CH_3)(CN)$ exhibits all five of the expected bands in the $5d^{10}$ region of 16–20 eV.[10a] In Figure 4 we present the calculated ionization energies, both nonrelativistic and relativistic. The results again show good agreement between experiment and theory. The first and fourth bands are extremely sharp and on that basis they were assigned to the spin–orbit split components of the d_δ ionization.[10a] This is in apparent agreement with the calculated results, although due to the lower symmetry of this complex (C_{3v}) the d orbitals belong to only two representations (a_1 and e), and in the double group there are also only two representations (S1 and S3). We have not carried out an eigenvector analysis for $(CH_3)Hg(CN)$, so that the predominant character of the ion states presented in Figure 4 is based on the experience we gleaned from out studies on $Hg(CN)_2$ and $Hg(CH_3)_2$. With only one CN group replacing a CH_3, the $5d_\sigma$ does split off to 3S1, not as far down as in $Hg(CN)_2$, but much further than the original assignment indicated.[10a]

For reference purposes the calculated ionization energies (eV) including relativistic effects for $Hg(CH_3)(CN)$ are[21]

a_1(S1) 26.0, 20.0, 18.0, 13.5, 11.5, 10.0

e(S3) 18.1, 16.5, 13.5, 11.5

e(S1) 17.0, 16.4, 13.5, 11.5

The Mulliken population analysis of the orbitals (not presented) shows that the Hg 6s character is spread over $4a_1$, $5a_1$, and $6a_1$; hence the mass–velocity correction to each of these orbitals is small. The MO $4a_1$ is mainly Hg–CN, $5a_1$ is σ CN, and $6a_1$ is Hg–CH_3. In the e representation, 3e is almost pure CH_3(1e) and 4e is CN(1π). The destabilization of π CN relative to e CH_3 appears to be due to the fact that the CN ligand has a calculated charge of −0.41 whereas the CH_3 ligand is only −0.16.

(4) $Hg(CCCH_3)_2$. The UP spectrum of $Hg(CCCH_3)_2$ in the $5d^{10}$ region exhibits five bands.[10b] In Figure 5 we compare our calculated IEs with experiment. The agreement is very good, with the Hg 5d experimental IEs calculated to within a few tenths of an electron volt. We also note that the sequence of ion states is calculated exactly the same as for $Hg(CH_3)(CN)$, in agreement with the close similarity between the UP spectra of the two compounds. The lowest d-type ionization event is now designated S5 rather than S1 due to the higher symmetry of $Hg(CCCH_3)_2$ compared to $Hg(CH_3)(CN)$. The components containing a large amount of d_δ character are again assigned to the first and fourth bands, in agreement with the experimental assignment. However, the fifth ionization event is predicted to be S1 and to correspond to ionization of an orbital that is predominantly d_σ in character. This latter prediction is based on the fact that in the ground-state calculation,[22] the $3a_1'$ orbital lies almost 1.5 eV more stable than 1e″, through which it couples in the spin–orbit matrix. As seen in the case of $Hg(CN)_2$, this amount of splitting is sufficient to severely decouple the components. Hence the 3S1 ionization event must be due to ionization of the d_σ orbital, in distinct contrast

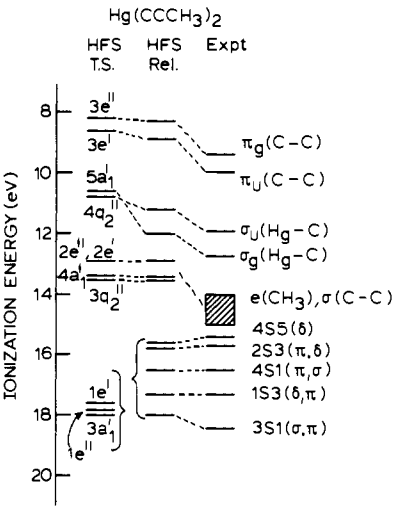

Figure 5. Correlation between theory and experiment for $Hg(CCCH_3)_2$.

to the assignment arrived at by analogy with $Hg(CH_3)_2$.[10b]

In this case we also can compare the experimental and theoretical IEs for the low ionization bands since the complete spectrum is reported. There is good agreement in this region of the spectrum also, except that our calculated IEs are too low in each case by about 3/4 eV. The Mulliken population analysis shows that the π^* orbitals of the propynyl ligand interact only slightly with the Hg $5d_\pi$ orbitals so that the resulting π^* ligand population is only 0.02 electrons. For reference purposes our calculated IEs (eV) including relativistic effects are[23]

a_1'(S1) 18.0, 13.4, 12.0

a_2''(S5) 13.6, 11.2

e′(S5) 15.6, 12.9, 8.9

e′(S3) 17.3, 12.9, 8.9

e″(S3) 15.8, 12.9, 8.3

e″(S1) 16.6, 12.9, 8.3

We can now summarize our results on the Hg compounds by pointing out that the mixing of the d_σ orbital with the other 5d orbitals strictly depends upon the competition between the spin–orbit and ligand-field effects. The spin–orbit effects are more important for $Hg(CH_3)_2$, but for the other compounds the ligand field effect is the more important factor. We now turn to the situation with the Au compound to see which factor will be most important in that case.

(5) $Au(PMe_3)(CH_3)$. The He(I) and He(II) UP spectra of $Au(PMe_3)(CH_3)$ have been reported.[11] In the He(II) spectrum the peaks at 9.84, 10.55, and 11.33 eV exhibit an increase in relative intensity and are therefore logically assigned to ionization events involving the Au 5d orbitals. The first two peaks at 8.24 and 9.22 eV were assigned to ionizations from the Au–C and Au–P orbitals, respectively, based on the results of the Xα-SW calculations.[11] The remainder of the spectrum from 12 eV onward is a series of overlapping peaks due to the host of ionizations involving the e(CH_3) and a_1(CH_3) orbitals of the PMe_3 ligand.

One of the interesting features of this gold compound is that it clearly has at least three of the five d-type ionizations to low energy and close to the assigned IE of the Au–P bond. Also, we suspect that the e(CH_3) IE of the unique CH_3 is very close in energy to that of the d IEs in view of the low onset of such ionization events in, for example, $W(CH_3)_6$.[24] This is quite different than the situation for $Hg(CH_3)_2$, where the CH_3 ioni-

(20) Jonkers, G.; De Lange, C. A.; Noodleman, L.; Baerends, E. J. *Mol. Phys.* **1982**, *46*, 609.

(21) The two a_1 ionization energies at 26.0 and 20.0 eV were obtained from an average of results from the upper four a_1 transition-state calculations.

(22) As in footnote 19, the ground-state spinor analysis turns out to be adequate for this compound.

(23) Except for those ionization events involving the d band, we have applied ground-state relativistic corrections to the transition-state energies.

(24) Green, J. C.; Lloyd, D. R.; Gayler, L.; Mertis, K.; Wilkinson, G. *J. Chem. Soc., Dalton Trans.* **1978**, 1403.

Table VIII. Mulliken Population Analysis for the Upper Occupied Orbitals of $Au(PMe_3)(CH_3)$

orbital	ionization energy	percent character[a] Au	PMe_3	CH_3
$5a_1$	12.00	49.9 $5d_\sigma$	26.9 a_1	6.5 $2a_1$
$6a_1$	8.13	12.8 6s	53.4 a_1	7.1 $2a_1$
		24.0 $5d_\sigma$		
$7a_1$	7.02	34.4 6s		57.7 $2a_1$
		6.0 $5d_\sigma$		
4e	11.86	8.4 $5d_\pi$	87.8 e	
5e	10.87	48.3 $5d_\pi$	9.6 e	40.1 e
6e	10.89	7.9 $5d_\pi$		18.4 e
		72.4 $5d_\delta$		
7e	9.76	29.8 $5d_\pi$		39.9 e
		26.9 $5d_\delta$		

[a] Occupations: Au, $(5d_\delta)^{2.00}(5d_\pi)^{1.94}(5d_\sigma)^{1.79}(6s)^{1.02}(6p_\pi)^{0.0}(6p_\sigma)^{0.0}$; PMe_3, $(4e)^{2.00}(4a_1)^{1.68}$; CH_3, $(1e)^{2.00}(2a_1)^{1.44}$. Fragment charges: Au, +0.20; PMe_3, +0.20; CH_3, −0.40.

zations occurred in the range 13–14.5 eV and the d ionizations occurred at 15–17 eV. Consequently, the gold complex offers unique advantages to study the possible increase in d orbital involvement in bonding compared to mercury compounds.

We have completed HFS calculations on both $Au(PH_3)(CH_3)$ and on $Au(PMe_3)(CH_3)$. The overall eigenvalue spectrum and the calculated orbital character was not appreciably different for the upper occupied valence MOs (top three a_1 and top three e). However, as we became interested in the precise details of the UP spectrum, we decided to carry out a complete set of calculations on the PMe_3 complex, and we report these results here rather than our calculations on the model PH_3 complex.

A ground-state energy level diagram is presented in Figure 6, along with the calculated transition-state IEs and the shifts brought about by relativistic effects. Once again there is excellent overall agreement between theory and experiment. Due to the high-lying position of the Au 5d orbitals compared to Hg 5d and the low-lying PMe_3 donor orbital compared to that of CH_3, the Au $5d_\sigma$ and PMe_3 a_1 orbitals lie close together in energy. This results in a strong interaction and stabilizes the d_σ orbital at the nonrelativistic level. Even with the relativistic corrections, we still predict a spinor with a large component of d_σ to be the last of the five ionization bands expected from the Au 5d orbitals. In fact, we predict it to lie under the broad band that begins at 12 eV. In the prediction of a relatively high IE for the ionization event involving a large component of d_σ for $Au(PMe_3)(CH_3)$, it is similar to $Hg(CN)_2$, $Hg(CH_3)(CN)$, and $Hg(CCCH_3)_2$.

The second important feature that we notice in Figure 6 is that the $e(CH_3)$ and Au 5d levels do lie close together in energy and that there is extensive mixing of these fragment orbitals to form the 5e, 6e, and 7e MOs. This qualitative analysis is borne out by the population results presented in Table VIII. We further notice from Table VIII that the Au $5d_\sigma$ orbital population is only 1.8 electrons compared to values close to 1.9 that were found for

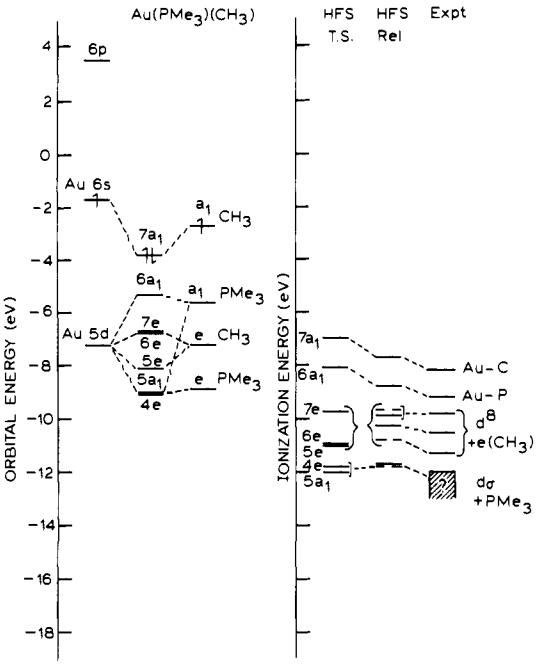

Figure 6. Orbital energy level diagram and calculated ionization energies for $Au(PMe_3)(CH_3)$.

the corresponding orbital in the Hg compounds. This may lead us to suspect that the Au 5d orbital is more involved in bonding than Hg 5d, but that factor will be examined more thoroughly in section B.

In Table IX we display the transition state and relativistic shift effects for the upper occupied a_1 and e MOs. As a result of differential relaxation effects, the 5e and 6e IEs are calculated to be nearly identical at the nonrelativistic level. The relativistic effects bring about a severe mixing of the 6e and 7e MOs as seen from the relativistic eigenvector analysis (Table X). The final calculated IEs for 5e, 6e, and 7e all lie within about 1.2 eV. Consequently, we assign the six resultant ionization events from these three MOs to the three experimental bands that occur at 9.84, 10.55, and 11.33 eV. The assignment presented in Figure 6 is the most logical one and is not inconsistent with the relative intensities of the bands observed in the experimental spectrum.[11] In other words, the qualitative assignment of these three ionization bands is "d^8 + $e(CH_3)$". The eigenvector analysis (Table X) shows that the 9S1 state consists mostly of the $5a_1$ MO, which is mainly the $5d_\sigma$ orbital (Table VIII). In fact, the $5d_\sigma$ ionization event is calculated to lie slightly more stable than one of the ionizations involving the 4e MO, which is mainly PMe_3 in character. As in the case of all the Hg compounds except $Hg(CH_3)_2$, the ionization event involving the major component of the $5d_\sigma$ orbital is predicted to lie more stable than originally assigned.[11] Closer examination of the meaning of this for bonding is presented in section B.

Table IX. Summary of Nonrelativistic and Relativistic HFS Calculations for the Upper Occupied Orbitals of $Au(PMe_3)(CH_3)$[a]

	nrel	Δ_{MV}	Δ_{DAR}	Δ_{SO}	Δ_{SO}^{ind}	Δ_{POT}	rel	rel state
$5a_1$	−12.00	−1.07	0.24	0.00	−0.30	1.32	−11.81	9S1
$6a_1$	−8.13	−1.38	0.57	0.00	−0.03	0.20	−8.77	14S1
$7a_1$	−7.02	−2.26	1.07	0.00	0.00	0.49	−7.72	15S1
4e	−11.86	−0.05	0.00	−0.01	−0.21	0.34	−11.79	10S1
		−0.05	0.00	0.01	−0.01	0.22	−11.69	4S3
5e	−10.87	−0.64	0.02	−0.10	−0.43	1.12	−10.90	11S1
		−0.64	0.02	0.10	−0.62	1.12	−10.89	5S3
6e	−10.89	−1.24	0.04	0.35	0.12	1.76	−9.86	12S1
		−1.24	0.04	−0.35	−0.05	2.15	−10.34	6S3
7e	−9.76	−0.69	−0.01	−0.08	−0.13	0.98	−9.69	13S1
		−0.69	−0.01	0.08	0.24	0.92	−9.22	7S3

[a] Footnotes as in Table III.

Table X. Percent Analysis of the Relativistic Spinors for the Ground-State Calculation on $Au(PMe_3)(CH_3)$

state	$5a_1$	$6a_1$	$7a_1$	$4e_1$	$4e_2$	$5e_1$	$5e_2$	$6e_1$	$6e_2$	$7e_1$	$7e_2$
9S1	92.6			3.5	3.5						
10S1				42.9	42.9			2.3	2.3		
11S1						45.4	45.4			2.4	2.4
12S1		34.0				2.2	2.2			30.0	30.0
13S1		58.3						6.8	6.8	12.7	12.7
14S1		6.2	14.9					33.4	33.4	4.0	4.0
15S1			82.4					4.7	4.7		
4S3				49.5	49.5						
5S3						43.6	43.6			4.8	4.8
6S3						2.1	2.1	28.2	28.2	19.6	19.6
7S3						4.3	4.3	20.3	20.3	25.2	25.2

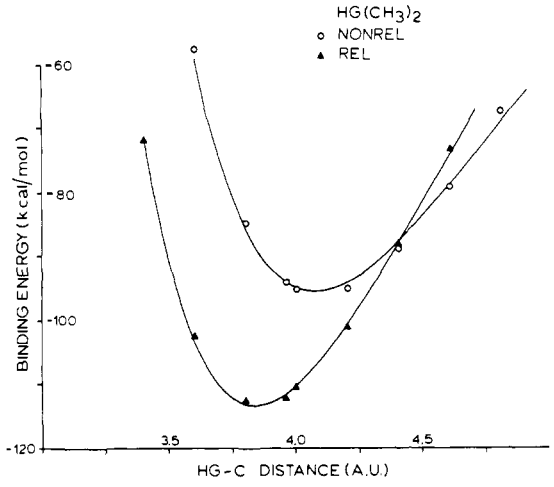

Figure 7. Calculated potential energy curves with and without relativistic effects for $Hg(CH_3)_2$.

There is one method[25] involving a combination of experimental data and empirical analysis of it that would allow a test of our prediction that the $e(CH_3)$ MO lies in the region of the Au 5d ionizations. This method requires a comparison of the C1s core IEs of the methyl C atom bound to the Au atom with the corresponding IE for a "model" compound, in this case most probably CH_4. Then the $e(CH_3)$ IE is predicted to shift 0.8 times the amount of the shift in the C1s IE. The C1s core IE has not been reported for the gold complex. One of the difficulties with this approach for the present gold compound is that it may prove impossible to experimentally resolve the C1s IE of the methyl groups attached to the P atom as compared to that attached to the Au atom.

(B) Relative Participation in the Bonding by Metal 5d, 6s, and 6p Orbitals. As mentioned in the introduction, the relative contribution to bonding by the three types of valence metal orbitals is an unknown quantity. Within the framework of the Ziegler transition-state energy analysis,[18] we are able to examine the detailed nature of the bonding for these compounds.

(1) $Hg(CH_3)_2$. We first examine the calculated binding energy for $Hg(CH_3)_2$, with and without relativistic corrections. The results are presented in Figure 7, where the energy scale is with respect to the Hg atom and two planar, unrestricted CH_3 groups. It is seen that the relativistic correction contracts the equilibrium bond length by only about 0.1 Å, but the binding energy changes significantly. The calculated equilibrium bond length is very near the experimental value of 3.9571 au (2.09 Å).

The binding energy with respect to Hg and CH_3 fragments has been calculated at the experimental Hg–C bond length and is here discussed on a per $(Hg–CH_3)$ bond basis. At the nonrelativistic level the binding energy with respect to spin-restricted pyramidal CH_3 fragments is 71.5 kcal/mol. Allowing the free ligand CH_3 fragment to be planar[26] provides a stabilization of 14.6 kcal/mol, and a further stabilization of 9.8 kcal/mol results from doing the calculation spin unrestricted; the corrected nonrelativistic binding energy is 47.1 kcal/mol. The relativistic correction is 9.1 kcal/mol so that the final calculated Hg–CH_3 bond strength is 56.2 kcal/mol. This number is to be compared with the experimental value of 57.5 kcal/mol—the energy required to remove the first CH_3 ligand from $Hg(CH_3)_2$.[15a] A more realistic comparison is with the standard enthalpy of dissociation to Hg_g and $2CH_{3g}$; this value is 58 kcal/mol or 29 kcal/mol of Hg–CH_3 bonds.[15b]

Table XI. Decomposition of the Total Bond Energy between Hg and $CH_3\cdots CH_3$ at the Nonrelativistic Level (kcal/mol)[a]

term	Hg 5d in valence	Hg 5d in core
$\Delta E(2H_3C\cdot \rightarrow H_3C\cdots CH_3)$	+50.1	+50.1
ΔE(steric)	−5.7	−5.7
$\Delta E(a_1')$	−123.8	−109.3
$\Delta E(a_2'')$	−8.8	−8.6
$\Delta E(e')$	−3.6	−3.7
$\Delta E(e'')$	−2.4	−0.0
total nonrelativistic	−94.2	−77.2

[a] The $\Delta E(2H_3C\cdot \rightarrow H_3C\cdots CH_3)$ term represents the energy required to go from a planar (unrestricted) $\cdot CH_3$ radical to $H_3C\cdots CH_3$ at the $Hg(CH_3)_2$ geometry and with the excited $(a_1')^0(a_2'')^2$ configuration for the odd electrons (see text).

We next turn to a detailed analysis of the binding in $Hg(CH_3)_2$ in terms of *steric* and *electronic* interaction between fragments. In order to properly do the analysis, we must have closed-shell fragments. Hence, we choose as our fragments an Hg atom and a single ligand fragment consisting of $CH_3\cdots CH_3$ at the bond length appropriate for "insertion" of the Hg atom. For the ligand fragment the frontier CH_3 orbitals $(2a_1')$ combine to form symmetric (a_1') and antisymmetric (a_2'') orbitals. Obviously, the more stable orbital is a_1', but we choose to pair up the odd electrons of CH_3 in the orbital of a_2'' symmetry in the D_{3h} point group. This electron occupation places the "stretched" ligand in an excited configuration (19.9 kcal/mol). However, such an occupation allows the insertion of the Hg atom with no net change in the number of orbitals occupied in each symmetry. The occupied a_2'' orbital of the "prepared" ligand is available to interact with the empty $6p_\sigma$ orbital of Hg, and the unoccupied a_1' can receive electrons from the filled Hg 6s orbital. This excited-state, stretched ligand is repulsive with respect to two restricted, pyramidal CH_3 groups by 1.3 kcal/mol.

In Table XI we present the fragment energy analysis for $Hg(CH_3)_2$, for calculations both with and without the 5d orbital in the core. We examine first the results with 5d electrons in the valence shell. Notice that the steric interaction term is slightly negative, as a result of taking an excited state for the ligand fragment. The electronic interaction terms show that the major part of the bonding has occurred in the a_1' representation. This is the representation to which the Hg 6s orbital belongs. Only about 6% of the bonding is provided by the a_2'' representation, containing the Hg 6p orbital. Negligible bonding is contributed by the d_π and d_δ representations (e'' and e'). These energy results are in agreement with the qualitative results that we gleaned from the Mulliken population analysis in Table II.

(25) Jolly, W. L.; Eyermann, C. J. *J. Phys. Chem.* **1982**, *86*, 4834.
(26) Herzberg, G. *Proc. R. Soc. London* **1961**, *291*, 262.

Table XII. Decomposition of the Total Bond Energy between Hg and NC···CN at the Nonrelativistic Level (kcal/mol)[a]

term	Hg 5d in valence	Hg 5d in core
ΔE(2NC· → NC···CN)	+41.7	+41.7
ΔE(steric)	+10.2	+10.2
$\Delta E(\sigma_g)$	−190.9	−175.0
$\Delta E(\sigma_u)$	−10.4	−10.3
$\Delta E(\pi_g)$	−6.0	−0.1
$\Delta E(\pi_u)$	−5.8	−7.3
$\Delta E(\delta_g)$	−0.5	0.0
total nonrelativistic	−161.7	−140.8

[a] ΔE(2NC· → NC···CN) is the energy required to go from two ·CN radicals to NC···CN in the excited $(\sigma_g)^0(\sigma_u)^2$ configuration.

Turning now to the results presented in Table XI with the 5d orbitals in core, we see that the binding energy decreases only 12%. As expected, the majority of the binding energy loss has occurred in the a_1' representation. This indicates that what little binding was contributed by the 5d orbitals was due to the d_σ component.

We also have carried out calculations on $Hg(CH_3)_2$ without the use of Hg 6p orbitals. We observe that the HOMO a_2'' eigenvalue is destabilized by only 3.9 kcal/mol upon removing the 6p orbital from the basis set. The total binding energy changes by only 9.0 kcal/mol. These results, coupled with the small contribution to binding by the a_2'' representation as shown in Table XI, indicate that little binding is contributed by the Hg 6p orbitals. The binding in $Hg(CH_3)_2$ is best described in terms of a three-center 2-electron bond. We shall return to a more complete study of 6p orbital participation when we examine the bonding in $Hg(CN)_2$ presently.

(2) $Hg(CN)_2$. We have carried out a similar binding energy analysis for $Hg(CN)_2$ as that presented for $Hg(CH_3)_2$, and the results are given in Table XII. The major portion of the binding is due to the σ_g representation and the participation by the Hg 5d orbitals is negligible. Calculations without the use of Hg 6p show a destabilization of the σ_u orbital by only 2.5 kcal/mol, and the energy decreases by only 10.1 kcal/mol. Once again the major part of the binding is attributed to the Hg 6s orbital and the σ levels of CN. The total nonrelativistic binding energy per Hg–CN bond, after making the various corrections mentioned for $Hg(CH_3)_2$, is 80.8 kcal/mol. This is somewhat stronger than that calculated for $Hg(CH_3)_2$. No experimental bond strength has been reported for $Hg(CN)_2$.

We now examine more carefully the hypothesis that the Hg 6p orbital contributes little to the bonding in $Hg(CN)_2$ and $Hg(CH_3)_2$. The usual interpretation of the bonding is that the Hg atom undergoes sp hybridization in order to form bonds with two ligands.[9] The comparative bond strengths in MX_2 compounds where M is a group 2a or 2b metal atom and X is a halogen also have been cited as evidence for *n*p orbital involvement in such compounds.[27] For example, in the case of $HgCl_2$ the following bond dissociation energies have been reported (kcal/mol):[9]

$$HgCl_2 \xrightarrow[81]{} HgCl + Cl \xrightarrow[25]{} Hg + Cl + Cl$$

Such results, which are typical for group 2 metal halides, have been interpreted to indicate that whereas the Hg atom has an electronic configuration of s^2 in the free atom, it is sp hybridized in HgCl and $HgCl_2$. Consequently, the difference in the two bond dissociation energies must be due to s → p promotion energy on the Hg atom. Also, there are electron spin resonance data on a variety of MX and MH free radicals where M is a group 2 metal atom and X is a halogen. These ESR results have been interpreted to indicate a sizable *n*p orbital participation on the metal atom. In the case of HgH the (squared) coefficient of the 6p orbital in the MO containing the odd electron is thought to be around 0.50.[28] These results seem to be at odds with our contention that there is very little involvement of the Hg 6p orbital in the Hg compounds currently under investigation.

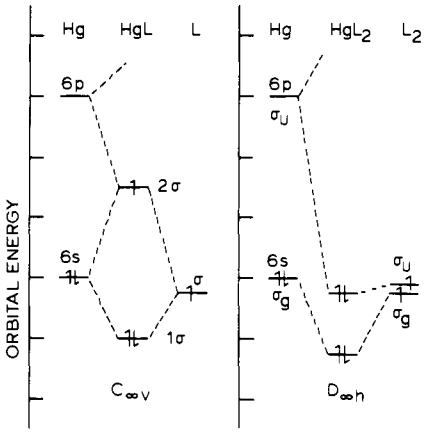

Figure 8. Schematic energy level diagram showing the relative importance of Hg 6p orbitals in HgL vs. HgL_2.

In order to examine the problem more closely, we also have completed HFS calculations on the free radical HgCN. The calculated binding energies at the nonrelativistic level, with and without 6p orbitals on the Hg atom, are presented herewith (kcal/mol):

$$Hg(CN)_2 \xrightarrow[\text{no 6p, } 124.6]{\text{with 6p, } 113.2} HgCN + CN \xrightarrow[\text{no 6p, } 26.9]{\text{with 6p, } 48.4} Hg + CN + CN$$

These results clearly show that the 6p orbital participation is important for the HgCN free radical, since the binding energy nearly doubles upon inclusion of the Hg 6p orbital. However, the 6p contribution to the binding energy for the first dissociation step of $Hg(CN)_2$ is small, indicating that 6p orbital involvement here is negligible. Our results for the 6p orbital coefficient in the MO containing the odd electron in HgCN are also in agreement with the reported results for HgH.[28] The calculated 6p orbital coefficient is 0.45 and the Mulliken population analysis shows 29.5% contribution.

The reason behind the lack of 6p involvement in HgL_2 but its importance for HgL is readily apparent from a simple σ MO diagram for the two species (Figure 8). In HgL, the odd electron occupies an antibonding MO, which tends to push it toward the 6p orbital. This has the effect of causing a significant amount of 6p orbital contribution, but at the same time the HgL bond is weakened due to the antibonding electron. On the other hand, the symmetry of HgL_2 is such as to remove the antibonding electron and place it along with the additional electron from L in the HOMO σ_u orbital, which is nonbonding, except for a small amount of bonding due to 6p orbital contribution. Thus, we see why the 6p orbital involvement in HgL_2 is so much less than that in HgL. The argument strictly revolves around the energetic closeness of the 6p orbital and the HOMO of the molecule in question. Our results would argue that this is a real phenomenon and not a calculational artifact. We have used a double ζ basis set, and the calculated s → p promotion energy for the Hg atom is very close to that observed experimentally.[8]

(3) Au(PMe_3)(CH_3). Finally, we turn to our bond energy calculations on the gold complex. As mentioned earlier, we carried out a complete set of calculations on both the full PMe_3 complex and on the model complex with the PH_3 ligand instead of PMe_3. There was no significant difference in the results for the upper occupied MOs that were analyzed in section A. However, because we were interested in the placement of the 9S1 ion state relative to the states predominantly derived from the PMe_3 ligand, we decided to do the calculations on the full complex. For the study in this section with respect to the relative involvement of 5d, 6s, and 6p orbitals, we have used the results from the model complex, since the computation time was considerably less.

Part of the reason that PH_3 serves as a good model for PMe_3 is that we have chosen both the HPH and CPC bond angles to

(27) Hildebrand, D. L. In "Advances in High Temperature Chemistry"; Eyring, L., Ed.; Academic Press: New York, 1967; Vol. 1, p 193.
(28) Knight, L. B., Jr.; Weltner, W., Jr. *J. Chem. Phys.* **1971**, *55*, 2061.

Table XIII. Decomposition of the Total Bond Energy between $AuCH_3$ and PH_3 (kcal/mol)

term	Au 5d in valence	Au 5d in core
ΔE(steric)	+10.3	+10.3
$\Delta E(a_1)$	-29.7	-20.8
ΔE(e)	-12.2	-3.7
total nonrelativistic	-31.6	-14.2
relativistic correction	-28.5	-23.2
relaxation of PH_3	+5.7	+5.7
total	-54.4	-31.7

be 105° in our calculations. The effect of changing the bond angle of PH_3 from its experimental value of 93 degrees to 105 degrees is quite dramatic on the lowest computed ionization energy: 10.23 vs. 9.41 eV, respectively. Since the experimental IE of PMe_3 is 8.62 eV,[11] the perturbed PH_3 ligand already is able to mimic this donor orbital aspect of the PMe_3 ligand.

Our binding energy results indicate the following energetics (including relativistic effects, kcal/mol):

$$Au(PH_3)(CH_3) \xrightarrow[\text{no 5d, 31.7}]{\text{with 5d, 54.4}}$$

$$Au(CH_3) + PH_3 \xrightarrow[\text{no 5d, not calculated}]{\text{with 5d, 78.5}} Au + PH_3 + CH_3$$

The breakdown of the energy terms with respect to the $Au(CH_3)$ and PH_3 fragments is presented in Table XIII both with and without 5d orbitals in the valence set for the first step of this reaction. We were particularly interested in determining whether there was more d orbital involvement in the gold compound than in the mercury compounds discussed earlier. Inspection of the results given in Table XIII shows that such is indeed the case. About 40% of the Au-PH_3 binding is lost upon removal of the Au 5d orbitals from the basis set. This is as expected, since the Au 5d orbitals are much more energetically available than the Hg 5d orbitals. Our calculations indicate that the Au 5d orbital involvement is large in contrast to the conclusions of Bancroft et al.,[11] based upon their interpretation of the UP spectra. The increased involvement of Au 5d over Hg 5d is in line with the lesser Mulliken population of the Au $5d_\sigma$ orbital compared to the Hg $5d_\sigma$ orbital (Tables II, V, and VIII).

Acknowledgment. This work was supported in part by financial aid from the Netherlands Organization for the Advancement of Pure Research (ZWO). R.D.K. also acknowledges the grant support of the Netherlands America Commission for Educational Exchange and of Calvin College for a Calvin Research Fellowship. We gratefully acknowledge helpful discussions with Dr. J. G. Snijders.

Registry No. $Hg(CH_3)_2$, 593-74-8; $Hg(CN)_2$, 592-04-1; $Hg(CH_3)(CN)$, 2597-97-9; $Hg(CCCH_3)_2$, 64705-15-3; $Au(PMe_3)(CH_3)$, 32407-79-7.

Protonation Equilibria and Charge Transport in Electroactive Tetracyanoquinodimethane Polymer Films

György Inzelt,[1] James Q. Chambers,* James F. Kinstle, and Roger W. Day

Contribution from the Department of Chemistry, University of Tennessee, Knoxville, Tennessee 37996-1600. *Received August 1, 1983*

Abstract: The electrochemical behavior and electron spin resonance response of thin films of tetracyanoquinodimethane polyester in contact with aqueous buffers have been studied. The results indicate that the coupling of electron- and proton-transfer steps in the classical 3 × 3 square scheme, which describes quinone electrochemistry, can significantly influence the charge-transport rate through the film, limiting the electroactivity to a fraction of the available electron-transfer sites and decreasing the effective diffusion coefficient for charge transport through the polymer film by 100-fold for specific conditions. The acid-base chemistry of the reduced acceptor sites in the film matrix accounts for the pH dependence of the voltammetric waves, the film passivation in acidic solutions, and the film dissolution at negative potentials in simple salt electrolytes. The acid dissociation constants of the reduced acceptor sites in the polymer matrix are estimated from the pH dependence of the $E_{1/2}$ values—for $TCNQH_2$ pK_a values of 6.9 ± 0.1 and 10 are obtained in aqueous phosphate buffers.

In the few years since the initial reports on the modification of electrodes with electroactive polymers,[2-4] the variety of systems studied, and the concomitant theories and applications, have mushroomed and are continuing to increase.[5] Intense interest has focused on electrocatalysis using polymer modified electrodes[6] and on electronically conducting polymer films based on poly(pyrrole),[7] poly(acetylene),[8] and related materials,[9] although other

Scheme I

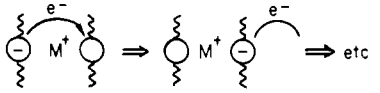

significant applications have appeared on the horizon. Included among the latter are electrochromic devices,[10] electrochemical desalination electrolysis,[11] neurotransmitter stimulating electrodes,[12] coatings for the stabilization of semiconductor photo-

(1) Deparptment of Physical Chemistry and Radiology, L. Eötvös University, Budapest, Hungary.
(2) Merz, A.; Bard, A. J. *J. Am. Chem. Soc.* **1978**, *100*, 3222.
(3) Van De Mark, M. R.; Miller, L. L. *J. Am. Chem. Soc.* **1978**, *100*, 3223.
(4) Kaufman, F. B.; Engler, E. M. *J. Am. Chem. Soc.* **1979**, *101*, 547.
(5) Albery, W. J.; Hillman, A. R. *R. Soc. Chem., Annu. Reports C* **1981**, *78*, 377.
(6) Anson, F. C.; Ohsaka, T.; Saveant, J.-M. *J. Am. Chem. Soc.* **1983**, *105*, 4883.
(7) Kanazawa, K. K.; Diaz, A. F.; Geiss, R. H.; Gill, W. D.; Kwak, J. F.; Logan, J. A.; Rabolt, J. F.; Street, G. B. *J. Chem. Soc., Chem. Commun.* **1979**, 854.
(8) MacInnes, D., Jr.; Druy, M. A.; Nigrey, P. J.; Nairns, D. P.; MacDiarmid, A. G.; Heeger, A. J. *J. Chem. Soc., Chem. Commun.* **1981**, *317*.
(9) (a) Chance, R. R.; Shacklette, G. G.; Miller, G. G.; Ivory, D. M.; Sowa, J. M.; Elsenbaumer, R. L.; Baughman, R. H. *J. Chem. Soc. Chem. Commun.* **1980**, 348. (b) Rabolt, J. F.; Clarke, T. C.; Kanazawa, K. K.; Reynolds, J. R.; Street, G. B. *Ibid.* **1980**, 347. (c) Waltman, R. J.; Bargon, J.; Diaz, A. F. *J. Phys. Chem.* **1983**, *87*, 1459. (d) Kaneto, K.; Kohno, Y.; Yoshino, K.; Inuishi, Y. *J. Chem. Soc., Chem. Commun.* **1983**, 382. (e) Shacklette, L. W.; Elsenbaumer, R. L.; Chance, R. R.; Sowa, J. M.; Ivory, D. M.; Miller, G. G.; Baughman, R. H. *Ibid.* **1982**, *361*.
(10) Desbene-Monvernay, A.; Lacaze, P. C.; Dubois, J. E.; Desbene, P. L. *J. Electroanal. Chem. Interfacial Electrochem.* **1983**, *152*, 87.
(11) Factor, A.; Rouse, T. O. *J. Electrochem. Soc.* **1980**, *127*, 1313.

0002-7863/84/1506-3396$01.50/0